Australasian Plant Pathology (2018) 47:431–447
https://doi.org/10.1007/s13313-018-0575-7

ORIGINAL PAPER

Three *Ganoderma* species, including *Ganoderma dunense* sp. nov., associated with dying *Acacia cyclops* trees in South Africa

J. M. Tchotet Tchoumi[1] · M. P. A. Coetzee[1] · M. Rajchenberg[2] · M. J. Wingfield[1] · J. Roux[3]

Received: 21 December 2017 / Accepted: 25 June 2018 / Published online: 29 June 2018

Abstract

Large numbers of *Acacia cyclops* trees are dying along the coastal plains of the Eastern and Western Cape Provinces of South Africa. The cause of the deaths has been attributed to a root and butt rot disease caused by the basidiomycete fungus *Pseudolagarobasidium acaciicola*. However, many signs (e.g. basidiomes) and symptoms reminiscent of Ganoderma root-rot are commonly associated with the dying trees. In this study, isolates collected from basidiomes resembling species of *Ganoderma,* as well as from root and butt samples from diseased *A. cyclops* trees were subjected to DNA sequencing and morphological studies to facilitate their identification. Multi-locus phylogenetic analyses and morphological characterisation revealed that three species of *Ganoderma* are associated with dying *A. cyclops* trees. These included *G. destructans*, a recently described species causing root-rot on trees elsewhere in South Africa. The remaining two were novel species, one of which is described here as *G. dunense*. The novel species is distinguished by its mucronate basidiomes, laccate shiny pileus surface, duplex context and ovoid basidiospores. Only an immature specimen was available for the second species and a name was consequently not provided for it. Interestingly, only a single isolate representing *P. acaciicola* was recovered in this study, suggesting that further investigations are needed to ascertain the role of each of the four basidiomycetous root-rot fungi in the death of *A. cyclops* trees.

Keywords Ganodermataceae · Phylogeny · *Pseudolagarobasidium* · Taxonomy · Rooikrans · Root rot

Introduction

Acacia cyclops A. Cunn.: G. Don (Fabaceae) is a woody shrub that occurs mainly in arid and coastal areas due to its ability to withstand severe environmental pressures such as drought, soil salinity and sand blasts (Gill 1985). In South Africa, the first trees of this species were introduced from Australia in the early 1830's to contain and stabilise the movement of sand dunes in the coastal areas of the country, including the Eastern and Western Cape Provinces (Avis 1989). Subsequently, the shrub developed rapidly to become an invasive weed and a serious environmental threat because it forms tall, thick, and almost impenetrable stands that stifle the establishment of native plants (Henderson 1998, 2007). However, despite being detrimental to the diversity of local plants, *A. cyclops* trees also provide an important source of firewood, charcoal and construction materials (Shackleton et al. 2006).

During the course of the last four decades, *A. cyclops* trees have been dying along the coastal planes in the Eastern and Western Cape Provinces of South Africa, particularly between the towns of George and Stilbaai (Taylor 1969; Wood and Ginns 2006; Kotzé et al. 2015). The dying trees suffer from a rapidly developing root and butt-rot disease that results in die-back, wilt, and a white rot of the affected roots and root collars. The disease has been attributed to the basidiomycete root-rot fungus *Pseudolagarobasidium acaciicola* Ginns (Wood and Ginns 2006; Kotzé et al. 2015). However, basidiomes of another fungus resembling a species of *Ganoderma* are also regularly seen attached to the bases of the dying trees. No attempt has been made to determine the identity of that fungus (Taylor 1969; Wood and Ginns 2006).

✉ J. Roux
Jolanda.roux@gmail.com

[1] Department of Biochemistry, Genetics and Microbiology, Forestry and Agricultural Biotechnology Institute (FABI), Faculty of Natural and Agricultural Sciences (NAS), University of Pretoria, Pretoria, South Africa

[2] Centro de Investigacion y Estension Forestal Andino Patagonico, Esquel, Chubut, Argentina

[3] Department of Plant and Soil Sciences, Forestry and Agricultural Biotechnology Institute (FABI), Faculty of Natural and Agricultural Sciences (NAS), University of Pretoria, Pretoria, South Africa

The genus *Ganoderma* P. Karst. (Basidiomycota, Polyporales, Ganodermataceae) has a worldwide distribution and includes both saprophytic and parasitic species. They cause white rot on a wide range of host trees (Flood et al. 2000), but are also of significant medicinal and cultural importance (Bishop et al. 2015). *Ganoderma* species are known to kill a wide variety of trees, including those with high economic value such as rubber (*Hevea brasiliensis* Müll.Arg.), tea [*Camellia sinensis* (L.) Kuntze], oil palm (*Elaeis guineensis* Jacq.) and ornamental and forest trees (Ramasamy 1972; Paterson 2007; Kinge and Mih 2011; Coetzee et al. 2015). They are also the main causal agents of root and butt rot diseases of numerous *Acacia* species in tropical regions of the world (Glen et al. 2009; Coetzee et al. 2011).

Identification and circumscription of species of *Ganoderma* has mainly relied on the description of morphological characteristics of the basidiomes, resulting in considerable taxonomic confusion (Richter et al. 2015). Most recently, the Phylogenetic Species Recognition (PSR) concept has improved species delimitation in the genus (Hong and Jung 2004; Zhou et al. 2015). Analyses of DNA sequences for loci such as the internal transcribed spacer (ITS: ITS1–5.8S-ITS2), the translation elongation factor 1-α (TEF1-α) and β-tubulin, among others, have facilitated the inference of relationships between species of *Ganoderma* (Park et al. 2012; Zhou et al. 2015; Xing et al. 2016). At least 438 specific and infraspecific names are listed for *Ganoderma* in Index Fungorum (http://www.indexfungorum.org/names/Names.asp, 08 July 2017). It has however, been suggested that less than one third of these names are valid (Kirk et al. 2008; Richter et al. 2015).

Studies by Taylor (1969) and Wood and Ginns (2006) revealed the recurring presence of basidiomes reminiscent of *Ganoderma* attached to the bases of dying *A. cyclops* trees in the Western Cape Province of South Africa. However, having demonstrated in pathogenicity trials that *P. acaciicola* was the causal agent of the tree death, the authors did not attempt to determine the identity of the *Ganoderma* species associated with the declining trees (Wood and Ginns 2006). The report of Wood and Ginns (2006) suggests that a single *Ganoderma* species is associated with dying *A. cyclops* trees although this might not be the case. The objective of this study was to resolve the identity of the unknown *Ganoderma* species occurring on declining *A. cyclops* trees using DNA sequence comparisons for multiple gene regions as well as morphological observations.

Materials and methods

Fungal collection and isolation

Basidiomes and recently infected roots and basal sections were collected from dying *A. cyclops*. Collection sites included areas close to the towns of Heroldsbaai and Stillbaai in the Western Cape Province and the Nelson Mandela Bay Metropolitan area (Port Elizabeth, PE) in the Eastern Cape Province (Fig. 1). Isolations were performed on a basidiomycete selective medium composed of 2% Malt Extract Agar (MEA) [20 g/L malt extract and 15 g/L agar, Biolab, Midrand, South Africa] supplemented with benomyl, dichloran and streptomycin (BDS) as outlined in Worrall (1991). Small pieces of wood (approximately 2–3 mm^3) from both infected basal sections and roots were first surface-disinfested in 7% bleach (NaClO) for ~ 90 s and rinsed twice with sterile distilled water before transferring them to the selective medium. Isolations from basidiomes were carried out by placing small sections (2–3 mm) obtained from the hymenophore onto the selective medium.

After 7–10 days of incubation at room temperature (22–24 °C), pure cultures were obtained by aseptically transferring small pieces of the growing margin of the fungal isolates onto fresh 2% MEA. Growth of the pure cultures was monitored for a further 7–10 days at room temperature (22–24 °C). Two mature cultures of each isolate were preserved in the culture collection (CMW) of the Forestry and Agricultural Biotechnology Institute (FABI), University of Pretoria, South Africa. Representative isolates were deposited in the culture collection (CBS) of the Westerdijk Fungal Biodiversity Institute, Utrecht, The Netherlands. Dried basidiomes were also deposited in the herbarium of the South African National Collection of Fungi (PREM), Roodeplaat, South Africa.

Genomic DNA extraction, amplification and sequencing

Genomic DNA was extracted from cultures (Table 1) following the Cetyltrimethylammonium Bromide (CTAB) extraction protocol described by Möller et al. (1992). DNA concentrations were determined with a NanoDrop® ND-1000 spectrophotometer (NanoDrop Technologies, Wilmington, DE, USA). Working DNA concentrations for polymerase chain reactions (PCRs) were obtained by adjusting the initial concentrations of the extracted genomic DNA to 100 ng/μL. The complete internal transcribed spacer (ITS) region, including ITS-1, ITS-2 and the 5.8S small subunit gene was amplified for all isolates using primers ITS1 and ITS4 (White et al. 1990). Amplifications of the partial translation elongation factor 1-α (TEF1-α) and partial β-tubulin gene regions were obtained using primer pairs EF595F/EF1160R (Kauserud and Schumacher 2001) and β-tubulin_F/β-tubulin_R (Park et al. 2012), respectively.

All PCR reactions were carried out in 25 μL total mixtures consisting of 17.5 μL sterile SABAX water (Adcock Ingram Ltd., Bryanston, RSA), 1 μL genomic DNA (100 ng/μL), 0.5 μL (2.5 units) of MyTaq™ DNA polymerase (Bioline), 5 μL 5 x MyTaq™ Reaction Buffer supplied with the enzyme

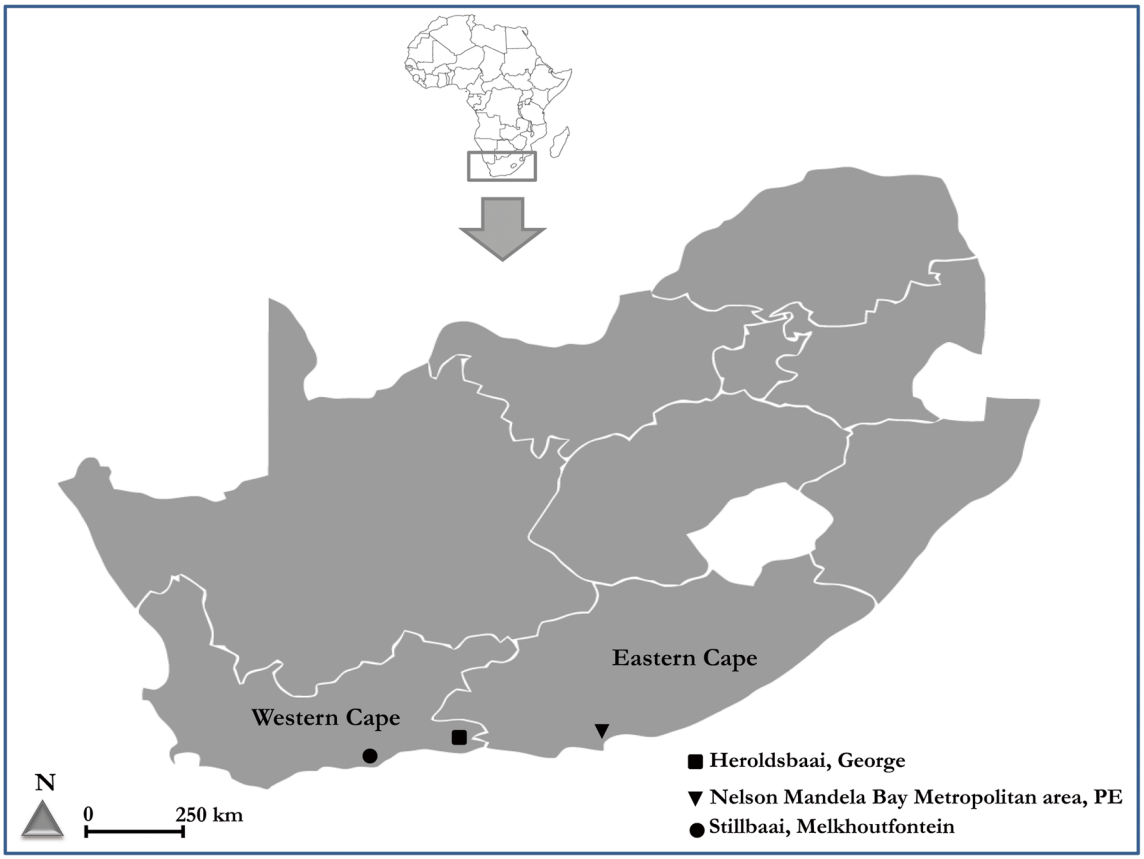

Fig. 1 South Africa map showing the sites in the Eastern and Western Cape Provinces where specimens of *Ganoderma* on *Acacia cyclops* were sampled. PE stands for Port Elizabeth

and 0.5 μL (10 mM) of each primer. The PCR conditions used with primers ITS1/ITS4 and EF595F/EF1160R were as follows: an initial denaturation step at 95 °C for 4 min, followed by 35 cycles of denaturation at 95 °C for 30 s, 30 s of annealing at 55 °C and 60 s of extension at 72 °C. The reactions were completed with a final elongation step at 72 °C for 7 min. Amplifications with the β-tubulin_F/β-tubulin_R primers were carried out with the same parameters as those used by Park et al. (2012). PCR products were electrophoresed on 2% agarose gels after staining with GelRed™ nucleic acid dye (Biotium Incorporation, USA) and visualized under UV illumination. Sephadex G-50 columns (Sigma, Steinheim, Germany) were then used to purify the PCR products following the recommendations of the manufacturer.

Purified PCR products were sequenced in 12 μL reaction volumes using the same primer pairs as in the amplification reactions. DNA sequencing reactions were done using Big Dye (Perkin-Emmer, Warrington, UK), following the protocol outlined by the manufacturer. Purification of the sequencing PCR products followed the same approach as for the PCR products. DNA sequencing was carried out on a DNA Analyzer ABI PRISM™ 3100 (Applied BioSystems, Foster City, CA, USA) at the sequencing facility of the University of Pretoria. CLC Main Workbench v7.6.1 was used to assess the quality of the electropherograms and to construct consensus sequences. DNA sequences of the β-tubulin and TEF1-α gene regions of *G. destructans* and *G. enigmaticum,* previously described from South Africa (Coetzee et al. 2015), were also generated for comparative purposes. These sequences as well as those of the novel species were deposited in GenBank (Table 1).

DNA sequence datasets and multi-gene phylogenetic analysis

Preliminary identification based on BLASTn searches of ITS sequences against those of reference sequences in GenBank was made to confirm that the sequences of the fungal isolates from *A. cyclops* were species of *Ganoderma.* Phylogenetic analyses were subsequently performed to determine the phylogenetic placement of the isolates from *A. cyclops*. For this purpose, four sequence datasets were generated. Of these, three represented the ITS, β-tubulin and TEF1-α gene regions alone, and one consisted of the combined sequences for all three loci. In addition to sequences generated in this study, the datasets also included reference sequences used in previous studies, including those of Glen et al. (2009), Douanla-Meli

Table 1 Isolates used in the phylogenetic analyses

Species	Voucher no.	Geographical origin	GenBank accession numbers		
			ITS	β-tubulin	TEF1-α
Ganoderma adspersum	Yao34456	United Kingdom	AJ006685	–	–
G. applanatum	Dai 12,483	China	KF494999	–	KF494977
G. applanatum	ATCC 44053	Japan	JQ520161	JQ675614	–
G. aridicola	Dai12588 (holotype)	South Africa	KU572491	–	KU572502
G. austroafricanum	CMW 41454	South Africa	KM507324	–	–
G. boninense	WD 2028	Japan	KJ143905	–	KJ143924
G. boninense	WD 2085	Japan	KJ143906	–	KJ143925
G. carnosum	MJ 21/08	Czech Republic	KU572492	–	–
G. carnosum	JV 8709/8	Czech Republic	KU572493	–	–
G. carnosum	CBS 516.96	Netherlands	–	JQ675616	–
G. cupreum	GanoTK4	Cameroon	JN105701	–	–
G. cupreum	GanoTK7	Cameroon	JN105702	–	–
G. curtisii	CBS 100131	United States of America (USA)	JQ781848	–	KJ143926
G. curtisii	CBS 100132	USA	JQ781849	–	KJ143927
G. curtisii	CBS 100132	Netherlands	–	JQ675617	–
G. destructans	CBS 139793 (type)	South Africa	NR132919	MG020151*	MG020213*
G. destructans	CMW 43671	South Africa	KR183857	MG020156*	MG020220*
G. destructans	CMW42129	South Africa	MG020232	MG020158	MG020191
G. destructans	CMW42130	South Africa	MG020233	MG020159	MG020192
G. destructans	CMW42131	South Africa	MG020234	MG020160	MG020193
G. destructans	CMW42134	South Africa	MG020235	MG020161	MG020216
G. destructans	CMW42135	South Africa	MG020236	MG020162	MG020214
G. destructans	CMW42136	South Africa	MG020237	MG020163	MG020194
G. destructans	CMW42137	South Africa	MG020238	MG020164	MG020195
G. destructans	CMW42138	South Africa	MG020239	MG020165	MG020196
G. destructans	CMW42139	South Africa	MG020240	MG020166	MG020197
G. destructans	CMW42140	South Africa	MG020241	MG020167	MG020215
G. destructans	CMW42141	South Africa	MG020242	MG020168	MG020198
G. destructans	CMW42142	South Africa	MG020243	MG020169	MG020199
G. destructans	CMW42143	South Africa	MG020244	MG020170	MG020221
G. destructans	CMW42146	South Africa	MG020245	MG020171	MG020200
G. destructans	CMW42147	South Africa	MG020246	MG020172	MG020201
G. destructans	CMW42148	South Africa	MG020247	MG020173	MG020202
G. destructans	CMW42151	South Africa	MG020250	MG020174	MG020203
G. destructans	CMW42152	South Africa	MG020251	MG020175	MG020204
G. destructans	CMW42153	South Africa	MG020252	MG020176	MG020205
G. destructans	CMW42154	South Africa	MG020253	MG020177	MG020206
G. destructans	CMW42155	South Africa	MG020254	MG020178	MG020217
G. destructans	CMW42158	South Africa	MG020256	MG020179	MG020224
G. destructans	CMW42159	South Africa	MG020257	MG020180	MG020223
G. destructans	CMW42160	South Africa	MG020258	MG020181	MG020207
G. destructans	CMW42161	South Africa	MG020259	MG020182	MG020208
G. destructans	CMW42162	South Africa	MG020260	MG020183	MG020209
G. destructans	CMW42163	South Africa	MG020261	MG020184	MG020218
G. destructans	CMW42164	South Africa	MG020262	MG020185	MG020210
G. destructans	CMW42165	South Africa	MG020263	MG020186	MG020211
G. destructans	CMW45109	South Africa	MG020266	MG020187	MG020225

Table 1 (continued)

Species	Voucher no.	Geographical origin	GenBank accession numbers		
			ITS	β-tubulin	TEF1-α
G. destructans	CMW45110	South Africa	MG020267	MG020188	MG020222
G. destructans	CMW45113	South Africa	MG020268	MG020189	MG020212
G. destructans	CMW45114	South Africa	MG020269	MG020190	MG020219
***G. dunense* sp. nov**	**CMW42149**	**South Africa**	**MG020248**	**MG020153**	**MG020226**
***G. dunense* sp. nov**	**CMW42150**	**South Africa**	**MG020249**	**MG020154**	**MG020228**
***G. dunense* sp. nov**	**CMW42157 (Type)**	**South Africa**	**MG020255**	**MG020150**	**MG020227**
G. gibbosum	XSD-35	Unknown	EU273514	–	–
G. gibbosum	AS5.624 type 3	China	AY593856	–	–
G. enigmaticum	Dai 15,970	Africa	KU572486	–	KU572496
G. enigmaticum	Dai 15,971	Africa	KU572487	–	KU572497
G. enigmaticum	CBS 139792 (type)	South Africa	NR132918	MG020157*	MG020231*
G. leucocontextum	Dai 15,601	China	KU572485	–	KU572495
G. leucocontextum	GDGM 44489	China	KM396271	–	–
G. lingzhi	Wu 1006–38 (holotype)	China	JQ781858	–	JX029976
G. lingzhi	Dai 12,574	China	KJ143908	–	JX029977
G. lingzhi	Dai 12,479	China	JQ781864	–	JX029975
G. lobatum	JV 0409/13 J	USA	KF605675	–	–
G. lobatum	JV 1212/10 J	USA	KF605676	–	KU572501
G. lobatum	ATCC 42985	Canada	–	JQ675618	–
G. lobatum	ASI 7061	USA	–	JQ675619	–
G. lucidum	Cui 9207	China	KJ143910	–	KJ143928
G. lucidum	K 175217	UK	KJ143911	–	KJ143929
G. lucidum	ASI 7117	Korea	–	JQ675633	–
G. lucidum	IUM 4303	Bangladesh	–	JQ675635	–
G. lucidum	IUM 0047	Korea	–	JQ675627	–
G. meredithae	ATCC 64492	USA	–	JQ675643	–
G. meredithae	ASI 7140	Unknown	–	JQ675644	–
G. mirabile	CBS 218.36	Philippines	–	JQ675645	–
G. multipileum	CWN 04670	China	KJ143913	–	KJ143931
G. multipileum	Dai 9447	China	KJ143914	–	KJ143932
G. multiplicatum	Dai 12,320	China	–	–	KU572500
G. multiplicatum	Dai 13,710	China	–	–	KU572499
G. mutabile	Yuan 2289 (type)	China	JN383977	–	–
G. neojaponicum	ASI 7032	Unknown	–	JQ675646	–
G. oerstedii	GO138	Unknown	–	DQ288098	–
G. oregonense	CBS 265.88	USA	JQ781875	NS	KJ143933
G. oregonense	ASI 7049	USA	–	JQ675647	–
G. oregonense	ASI 7067	USA	–	JQ675650	–
G. oregonense	CBS 266.88	USA	JQ781876	–	–
G. pfeifferi	CBS 747.84	Netherlands	–	JQ675651	–
G. philippii	E7098	Indonesia	AJ536662	–	–
G. philippii	E7092	Indonesia	AJ608710	–	–
G. resinaceum	BR 4150	France	KJ143915	–	–
G. resinaceum	CBS 194.76	Netherlands	KJ143916	–	KJ143934
G. resinaceum	ATCC 52416	Argentina	–	JQ675652	–
G. resinaceum	IUM 3651	Czech Republic	–	JQ675657	–
G. ryvardenii	HKAS 58055	Cameroon	HM138670	–	–

Table 1 (continued)

Species	Voucher no.	Geographical origin	GenBank accession numbers		
			ITS	β-tubulin	TEF1-α
G. ryvardenii	HKAS 58053 (type)	Cameroon	HM138671	–	–
G. sessile	JV 1209/9	USA	KF605629	–	KJ143936
G. sessile	LDW 20121017	USA	KJ143917	–	KJ143935
G. sinense	Wei 5327	China	KF494998	–	KF494976
***Ganoderma* sp.**	**CMW45100**	**South Africa**	**MG020264**	**MG020152**	**MG020229**
***Ganoderma* sp.**	**CMW45101**	**South Africa**	**MG020265**	**MG020155**	**MG020230**
Ganoderma sp.	ASI 7150	Unknown	–	JQ675665	–
Ganoderma sp.	ASI 7151	Unknown	–	JQ675666	–
G. subamboinense	GSUB136	Unknown	–	DQ288096	–
G. subamboinense	GSUB137	Unknown	–	DQ288097	–
G. tenue	GTEN24	Unknown	–	DQ288074	–
G. tornatum	CBS 109679	Netherlands	–	JQ675670	–
G. tornatum	BAFC1172	Argentina	AH008096	–	–
G. tornatum	BAFC1139	Argentina	AH008098	–	–
G. tropicum	He 1232	China	KF495000	–	KF494975
G. tropicum	Yuan 3490	China	JQ781880	–	KJ143938
G. tsugae	Dai 12751b	USA	KJ143919	–	KJ143939
G. tsugae	Dai 12,760	USA	KJ143920	–	KJ143940
G. tsugae	ATCC 64795	Canada	–	JQ675668	–
G. tsugae	ASI 7064	USA	–	JQ675669	–
G. valesiacum	CBS 428.84	USA	–	JQ675671	–
G. webeianum	CBS 219.36	Philippines	–	JQ675672	–
G. zonatum	FL-02	USA	KJ143921	–	KJ143941
G. zonatum	FL-03	USA	KJ143922	–	KJ143942
Tomophagus colossus	TC-02	Vietnam	KJ143923	–	KJ143943
Trametes suaveolens	–	Unknown	–	FJ410378	–

Reference sequences with star (*) are those generated in this study. In bold are isolates of the newly proposed species

and Langer (2009), Kinge et al. (2012), Park et al. (2012), Zhou et al. (2015), Coetzee et al. (2015), Xing et al. (2016) (Table 1). *Tomophagus colossus* (Fr.) C.F. Baker and *Trametes suaveolens* (L.) Fr. were selected as outgroup taxa. Sequence alignments were performed using the online version of MAFFT (http://mafft.cbrc.jp/alignment/server/index.html) v7 (Katoh and Standley 2013), and the phylogenetic relationships between taxa were evaluated using Maximum Likelihood (ML), Maximum Parsimony (MP) and Bayesian Inference (BI) analyses. The GTR + G + I substitution model determined by JModeltest v2.1.6 (Darriba et al. 2012) on CIPRES (Miller et al. 2010) under the Akaike Information Criterion (AIC) was selected as the best-fit nucleotide substitution model and incorporated in the phylogenetic analyses. Alignments and resulting phylogenetic trees were deposited in TreeBase (http://purl.org/phylo/treebase/phylows/study/TB2:S22037?x-access-code=fb98b1676b4efdbbc310326e01d0ad3c&format=htm).

Maximum likelihood analyses were performed in RaxML (Stamatakis 2006) using raxmlGUI 1.3 (Silvestro and Michalak 2012) with 10 parallel runs. Maximum likelihood bootstrap (MLB) analysis was done using 1000 replications. For BI analyses, four parallel runs, each with four Monte Carlo Markov Chains (MCMC) were performed using MrBayes v3.2 (Ronquist et al. 2012). Sampling of trees was carried out for four million generations with trees sampled at every 100th generation. The first 25% of the sampled trees were discarded as burn-in and the Bayesian posterior probabilities (BPP) were calculated for the remaining trees. Maximum Parsimony analyses were performed in PAUP* version 4.0b10 (Swofford 2002). A heuristic search option with a tree bisection-reconnection (TBR) branch swapping algorithm, involving 100 random stepwise additions of sequences, was used to generate the most parsimonious trees. All characters were of equal weight, gaps were treated as missing data and tree branches of zero length were collapsed.

The robustness of clades at the branch nodes was estimated using bootstrap (MPB) with 1000 replicates and using the same settings to obtain the fundamental tree but with the addition of sequences set to closest. Other estimated parameters included tree length (TL), consistency index (CI), retention index (RI), rescaled consistency index (RC), and homoplasy index (HI). The generated phylogenetic trees were visualized using MEGA 5.05 (Tamura et al. 2011).

Morphology

Microscopic observations were made from fine sections of basidiomes mounted on microscope slides in 5% KOH (potassium hydroxide) with and without 1% phloxine and Melzer's reagent (IKI). The observations were made using a Nikon Eclipse N*i* compound microscope (Nikon, Japan) at a magnification of up to 100× under an oil-immersion objective, and on a Zeiss Stemi SV6 stereo microscope. Images of the microscopic structures were captured with a Nikon DS-Ri2 camera fitted on the microscope and the measurements were made using the program NIS-Elements BR (Nikon Instruments Software-Elements Basic research).

Results

Signs and symptoms

Typical signs and symptoms of Ganoderma root rot (Glen et al. 2009; Coetzee et al. 2011; Gill et al. 2016) were observed on the declining *A. cyclops* trees. These included crown wilt and die-back, fresh basidiomes of *Ganoderma* attached to the bases of the affected trees (Fig. 2a), basal cankers and butt rot (Fig. 2b), and roots with reddish mycelial sheaths covering a whitish mycelial mat (Fig. 2c).

Fungal isolates

In total, 38 isolates resembling species of *Ganoderma* were obtained from a total of 55 diseased and dying trees. Of these, three were isolated from roots covered with the reddish mycelial sheaths; three from roots without the reddish mycelial sheaths; five from tree bases and the remaining 27 from fresh basidiomes (Table 1). The isolates in culture were either white to yellowish or completely yellow and ranged from having flat to fluffy mycelial growth.

DNA sequence comparisons

The ITS, β-tubulin and TEF1-α gene regions of the 38 isolates were successfully amplified using PCR, and DNA sequences were obtained for all the amplicons. Results of BLASTn searches based on ITS revealed that 36 isolates had a high level of DNA sequence similarity (99–100%) with *Ganoderma destructans*. Two others (CMW45100, CMW45101) had a high level of sequence similarity (99%) with *G. applanatum* (Pers.) Pat. and *G. gibbosum* (Blume & T. Nees) Pat. Besides the 38 *Ganoderma* isolates, a single isolate that was obtained from roots without rhizomorphic sheets was identified as *P. acaciicola*, and it was excluded from the rest of the study.

Fig. 2 Signs and symptoms of *Ganoderma* species infecting *Acacia cyclops* in South Africa. **a** Basidiome of *G. destructans* with reddish brown (laccate shiny) pilear surface attached to the base of wilting tree, **b** Collar rot, **c** Reddish brown to dark brown rhizomorphic sheet of a *Ganoderma* sp. covering root of dying tree

Sequence data and multi-gene phylogenetic analyses

The ITS dataset comprised of 89 ingroup taxa and one outgroup taxon. The dataset resulted in an alignment length of 651 characters, of which 357 were constant, 61 parsimony-uninformative and 233 parsimony-informative. The heuristic search resulted in eight parsimonious trees with TL = 540, CI = 0.622, RI = 0.899 and RC = 0.559. Since the tree topologies resulting from the BI, ML and MP analyses were nearly identical, only the ML tree is presented, along with the statistical values (BPP and Bootstrap values) of the two other analyses (Fig. 3). In the phylogenetic tree of the ITS sequence data, the isolates generated from *A. cyclops* formed two groups, clustering at distant positions. The first group, composed of 36 isolates, formed a monophyletic clade with isolates representing *G. destructans* and *G. multipileum*. This

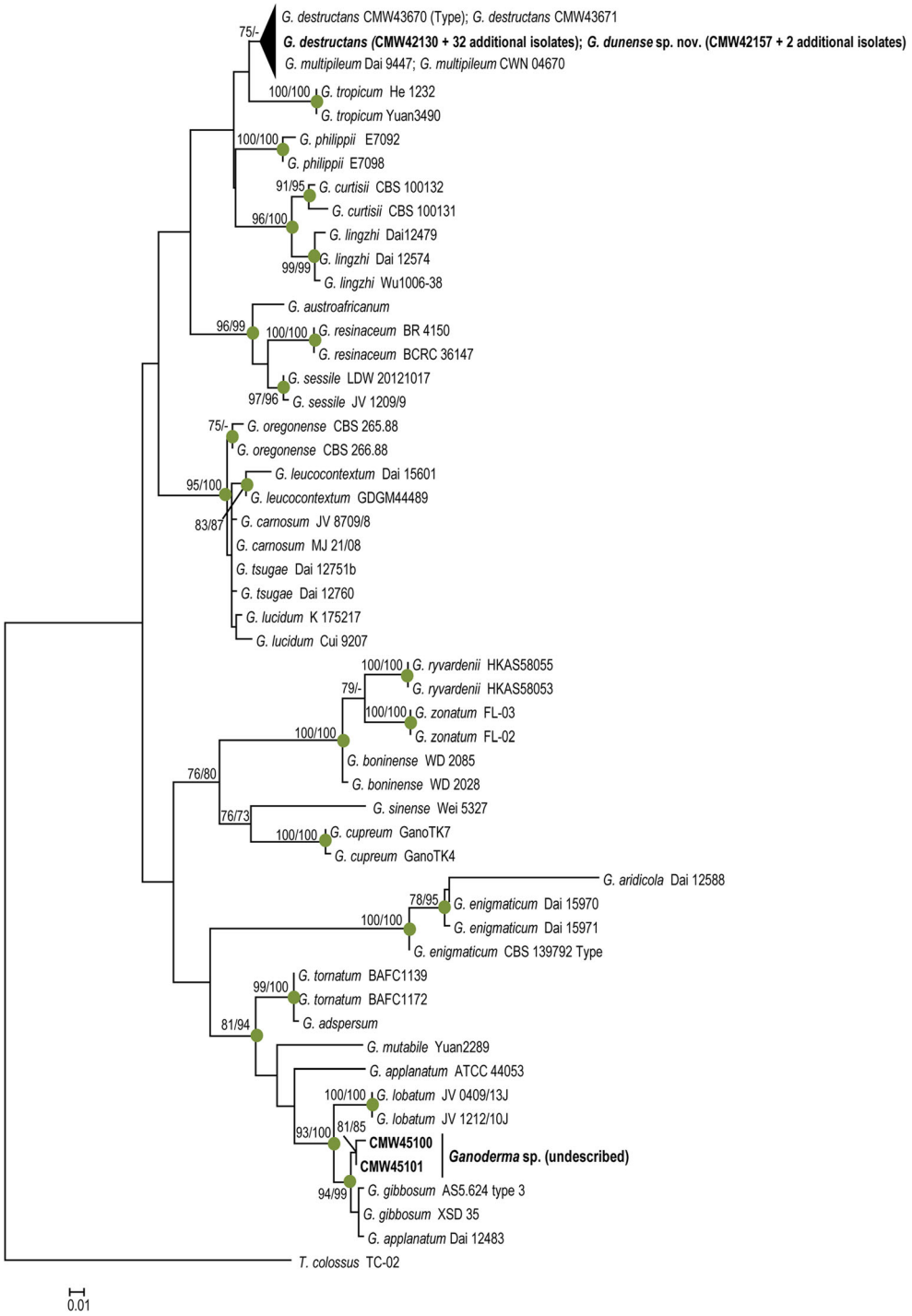

Fig. 3 Maximum likelihood tree based on ITS sequences, depicting the phylogenetic position of isolates obtained from *Acacia cyclops* (in bold) and related species within *Ganoderma*. Bootstrap values ≥70% from 1000 replicates of ML and MP analyses are displayed at the nodes. Posterior probability ≥0.95 from Bayesian Inference analysis are indicated at nodes with green circles

clade had statistical support only in the ML analysis (75% bootstrap support). The second group, comprised of isolates CMW45100 and CMW45101, nested in a strongly supported clade (MLB = 93%, MPB = 100% and BPP = 1) with isolates representing *G. applanatum*, *G. gibbosum* and *G. lobatum* (Schwein.) G.F. Atk. However, the two *A. cyclops* isolates formed a well-resolved sub-clade, although not sufficiently supported by BI analysis (BPP ≤ 0.95).

The β-tubulin sequence dataset consisted of 68 taxa, which resulted in an alignment length of 401 total characters. Of the total number of characters, 277 were constant, 44 were parsimony-uninformative and 80 parsimony-informative. The heuristic search yielded 100 parsimonious trees with TL = 206, CI = 0.544, RI = 0.887 and RC = 0.482. Only the ML consensus tree incorporating the statistical values of BI and MP is presented (Fig. 4) since the three analyses yielded

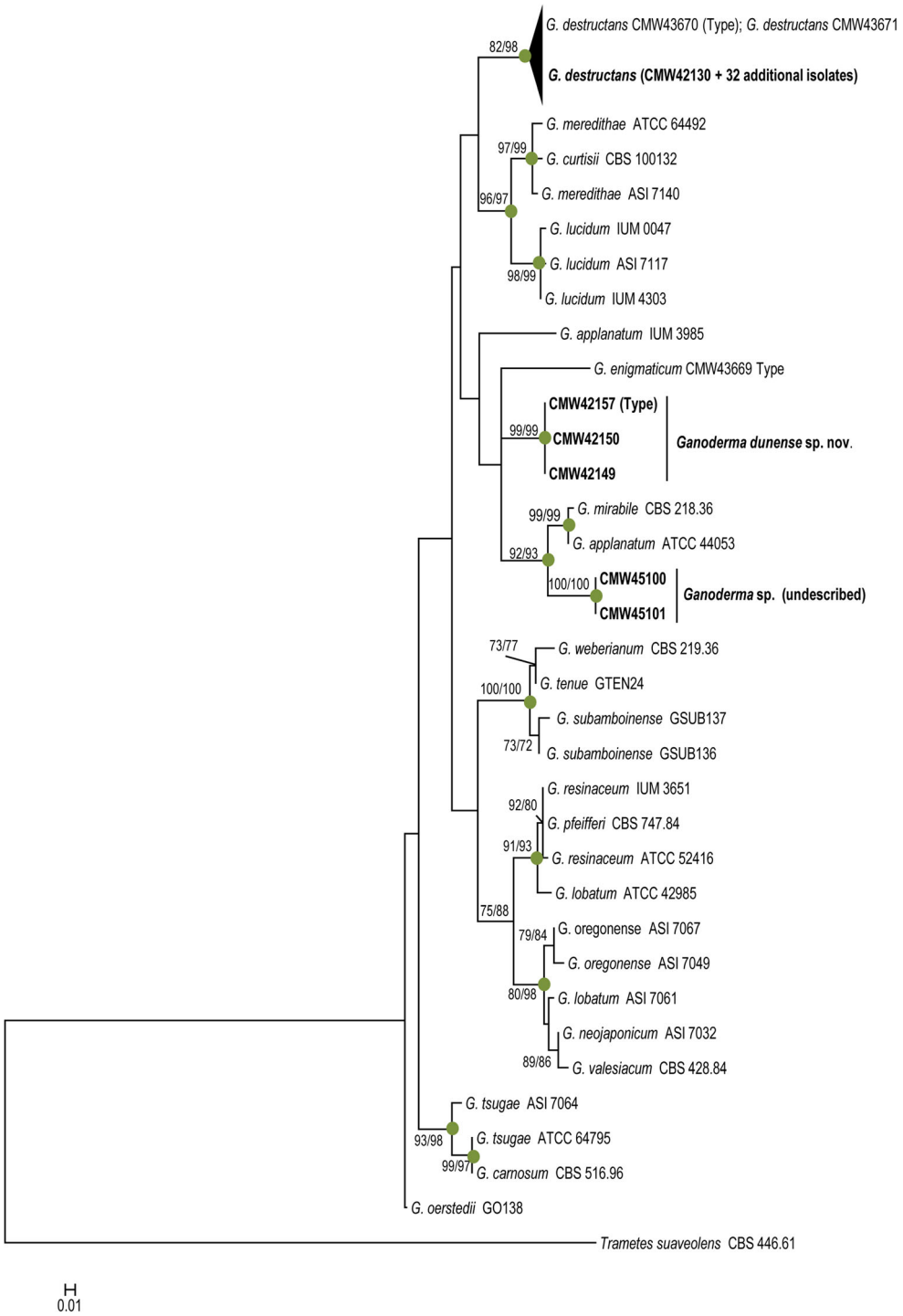

Fig. 4 Maximum likelihood tree based on β-Tubulin sequences, depicting the phylogenetic position of isolates obtained from *Acacia cyclops* (in bold) and related species within *Ganoderma*. Bootstrap values ≥70% from 1000 replicates of ML and MP analyses are displayed at the nodes. Posterior probability ≥0.95 from Bayesian Inference analysis are indicated at nodes with green circles

almost congruent topologies. In the β-tubulin phylogeny, unlike that for the ITS dataset, the isolates obtained from *A. cyclops* clustered at three different positions (Fig. 4). Thirty-three isolates (generated in this study) formed a monophyletic clade having strong statistical support with sequences representing *G. destructans* (MLB = 82%, MPB = 98%, BPP = 0.96). Three other isolates (CMW42149, CMW42150 and CMW42157) grouped in a well-resolved and strongly supported monophyletic cluster (MLB and MPB = 99%, BPP = 1), while the third group comprising isolates CMW45100 and CMW45101 formed another strongly supported clade (MLB and MPB = 100%, BPP = 1) that was closely related to the lineage including *G. mirabile* and *G. applanatum*.

The dataset from TEF1-α contained 71 ingroup taxa and one outgroup taxon. The total number of characters after alignment of the dataset was 579, of which 375 were constant, 35 were parsimony-uninformative and 169 parsimony-informative. The heuristic search resulted in 100 parsimonious trees with TL = 435, CI = 0.584, RI = 0.885 and RC = 0.517. The three analyses resulted in almost identical tree topologies. Hence, only the ML tree is shown alongside with BI and MP statistical values. As with β-tubulin, the TEF1-α phylogeny placed the isolates from *A. cyclops* at three different positions (Fig. 5). The first group, consisting of the same 33 isolates as in the β-tubulin gene tree, formed a strongly supported monophyletic clade (MLB = 99%, MPB = 100%, BPP = 0.98) with sequences representing *G. destructans* (generated in this study). This group was closely related to the lineage representing *G. multipileum*. The second group, including isolates CMW42149, CMW42150 and CMW42157, formed a well-supported monophyletic clade (MLB and MPB = 100%, BPP = 1). The third group of isolates, including CMW45100 and CMW45101, formed a cluster with *G. lobatum*, but represented a distinct lineage with high bootstrap values (MLB and MPB = 100%, BPP = 1).

The combined dataset of the ITS, β-tubulin and TEF1-α sequences comprised 115 taxa and 1631 total characters. In this dataset the ITS, β-tubulin and TEF1-α respectively contributed 651, 401 and 579 characters. Of the total number of characters, 1152 were constant, 94 parsimony-uninformative and 385 were parsimony-informative. The heuristic search generated 100 parsimonious trees with TL = 1005, CI = 0.541, RI = 0.878, and RC = 0.475. Since the three analyses resulted in similar topologies, only the topology of the ML, incorporating BPP and MP bootstrap values, is presented (Fig. 6). The phylogeny for the combined dataset supported that of β-tubulin and TEF1-α, placing the isolates obtained from *A. cyclops* at three different positions. A first group, consisting of the same 33 isolates as in the β-tubulin and TEF1-α phylogenies, formed a well-resolved monophyletic clade with strong statistical support (MLB = 88% and MPB = 98%) in ML and MP analyses with isolates representing *G. destructans*. This clade was closely related to *G. multipileum*, but both formed distinct lineages. The second group, comprised of isolates CMW42149, CMW42150 and CMW42157, clustered in a clearly resolved monophyletic clade with strong statistical support (MLB and MPB =100%, BPP = 1) in all three analyses. The third group, composed of isolates CMW45100 and CMW45101, formed a highly supported clade (MLB and MPB = 99%, BPP = 1), which was closely related to *G. lobatum* but with marginal support.

Taxonomy

Based on a phylogenetic species recognition concept, the 38 isolates of *Ganoderma* from *A. cyclops* in South Africa, represent three distinct taxa. One of these was *G. destructans* M.P.A. Coetzee, Marinc. & M.J. Wingf. (Coetzee et al. 2015) and two others represented novel species. One of these novel taxa (CMW45100 and CMW45101) is not described because only a rudimentary and immature basidiome (Fig. 7) could be found for it. The other new species, represented by isolates CMW42149, CMW42150 and CMW42157 is described as follows:

Ganoderma dunense Tchotet, Rajchenb., & Jol. Roux sp. nov.

MB823686.

Fig. 8

Etymology Name refers to the coastal sand dunes where this species was collected on dying *A. cyclops* trees.

Diagnosis *Ganoderma dunense* is morphologically similar to species in the *Ganoderma lucidum* complex. It is characterised by a light and spongy, perennial, applanate, dimidiate or reniform, mucronate basidiome, a laccate shiny pilear surface and a thick, soft-spongy duplex context. *Hymenial surface* poroid, white when fresh. *Hyphal system* trimitic and *basidiospores* ovoid, 10.9–12.3 × 7.3–8.5 μm, double walled with hyaline exosporium and yellowish brown coarse echinulae endosporium, IKI-.

Type South Africa, Western Cape Province, George, Heroldsbaai (S34° 03.242′ E22° 22.711′), at the base of dying *Acacia cyclops* A. Cunn. ex G. Don (Fabaceae), 13 April 2014, J.M. Tchotet Tchoumi and J. Roux, JMT137 (holotype-PREM61936, culture ex-type CMW42157 = CBS142831). GenBank accession number: ITS = MG020255, β-tubulin = MG020150, EF1-α = MG020227.

Description ***Basidiomes*** light, with spongy consistency, perennial, applanate, dimidiate or reniform, up to 14–20 cm wide, 11–15 cm radius, and 2–2.5 cm thick at base, mucronate; mucro lateral, more or less ellipsoid, 2.3–5 cm long, 1.8–4 cm wide. Margins more or less circular, slightly lobate and

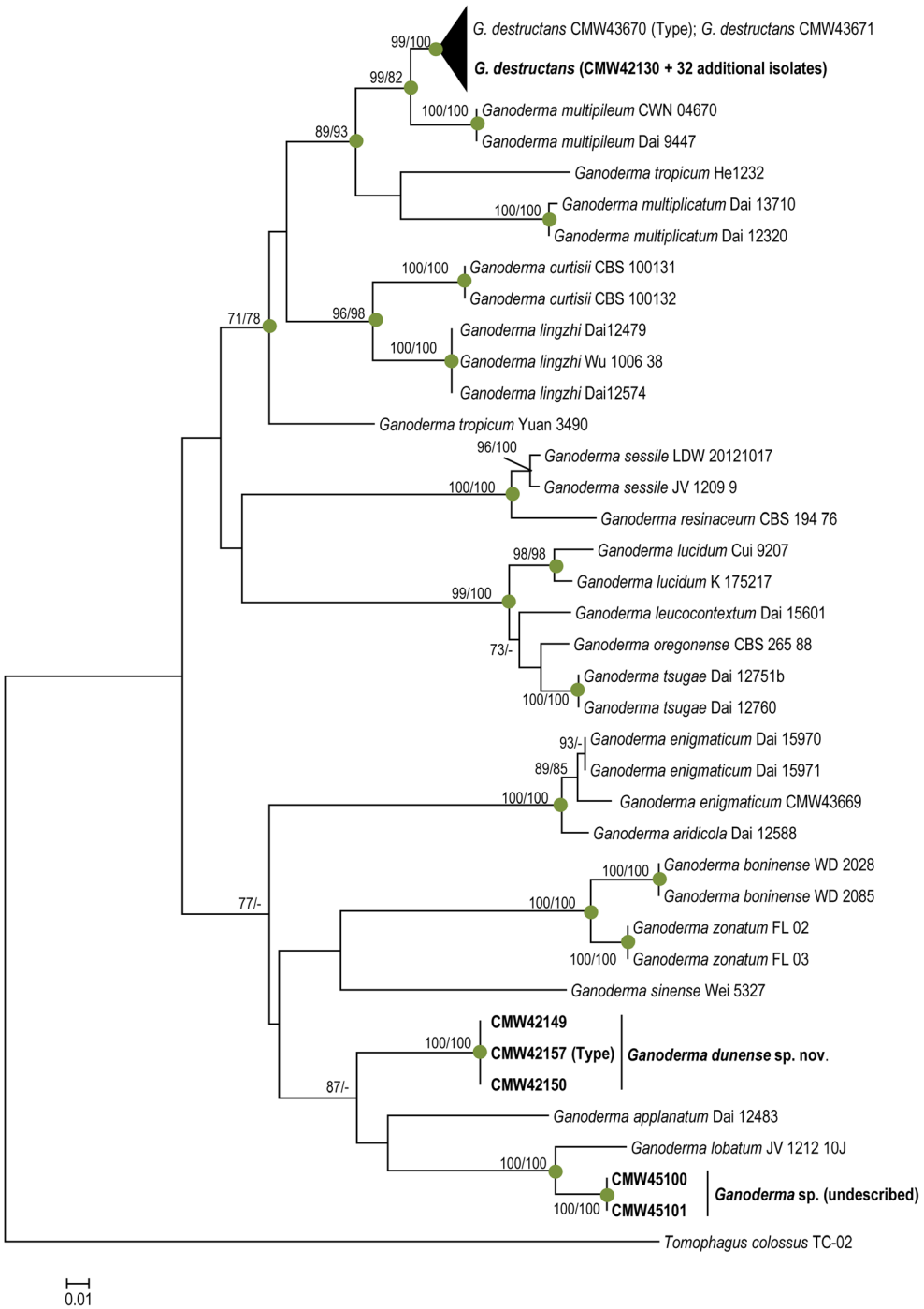

Fig. 5 Maximum likelihood tree based on TEF1-α gene sequences, depicting the phylogenetic position of isolates obtained from *Acacia cyclops* (in bold) and related species within *Ganoderma*. Bootstrap values ≥70% from 1000 replicates of ML and MP analyses are displayed at the nodes. Posterior probability ≥0.95 from Bayesian Inference analysis are indicated at nodes with green circles

round. ***Pileus surface*** laccate shiny, dark brown to dark brown chestnut, mostly covered by a dull brown deposit of basidiospores, glabrous, sulcate with wide furrows that become narrow towards the margins, and with irregular protuberances and a thin crust. ***Hymenial surface*** poroid, white when fresh turning brown to dark brown upon bruising; pores round to somewhat angular and elongated, 3–4 per mm; dissepiments thin. ***Context*** soft-spongy, 4–8 mm thick, duplex, with a light brown upper layer and a chocolate brown lower layer towards the tubes, absence of black resin-like deposits. ***Tubes*** light greyish brown, not stratified, up to 1.5 cm long. ***Hyphal system*** trimitic; generative hyphae not easily found, colourless, thin-walled, bearing clamp septa; skeletal hyphae poorly branched, brown to brown chestnut, thick-walled, 3.1–8 μm thick, lumen 1.4–2.2 μm wide; skeleto-binding hyphae present, branched at the apex with long flagelliform branches, basal stem unbranched. ***Cutis*** a hymeniodermis composed of a palisade of vertical and closely packed clavate cells; cells

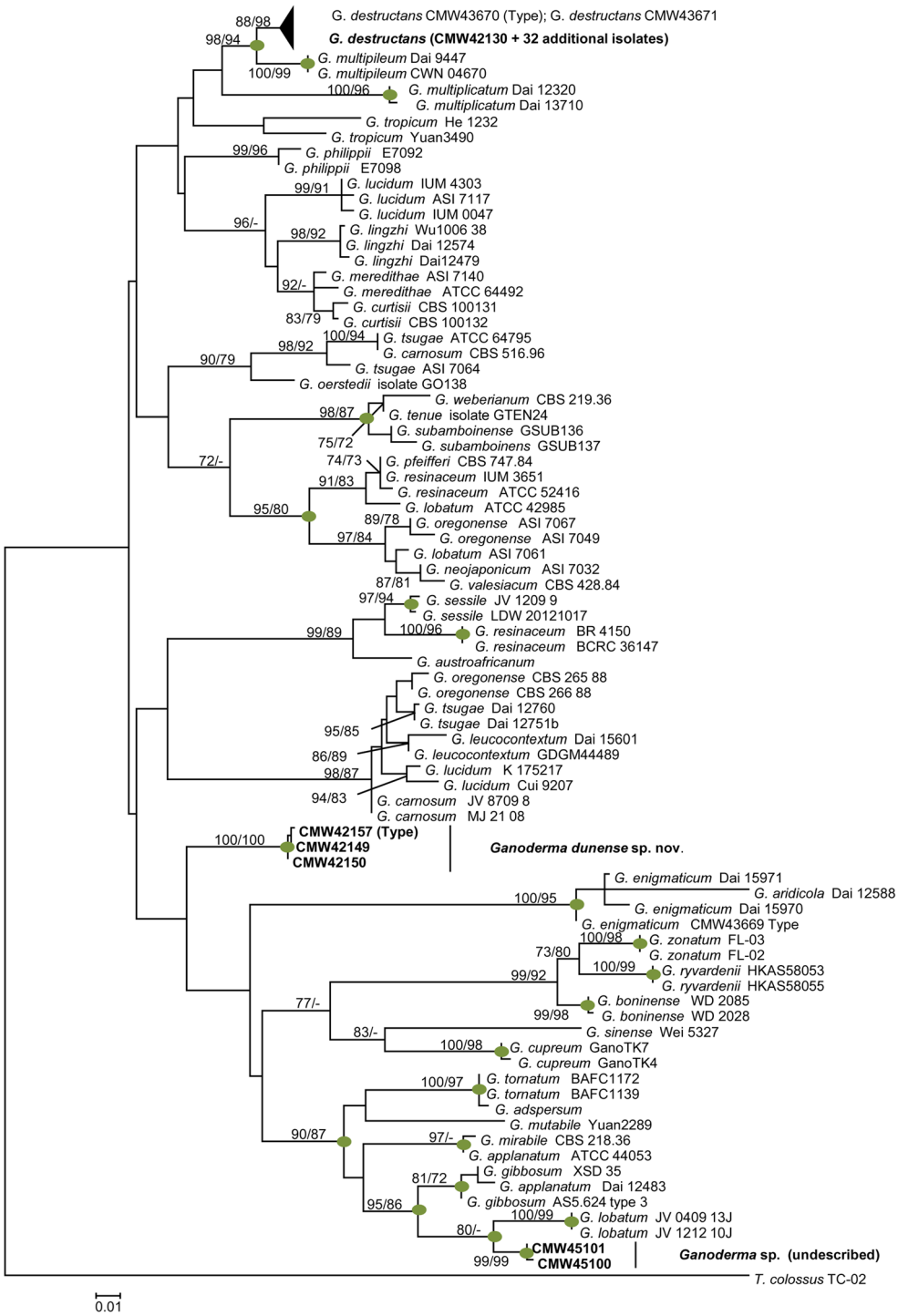

Fig. 6 Maximum likelihood tree based on combined dataset of ITS, β-Tubulin and TEF1-α gene sequences, depicting the phylogenetic position of the isolates obtained from *Acacia cyclops* (in bold) and related species within *Ganoderma*. Bootstrap values ≥70% from 1000 replicates of ML and MP analyses are displayed at the nodes. Posterior probability ≥0.95 from Bayesian Inference analysis are indicated at nodes with green circles

yellowish brown, thick–walled, some inflated at the apex and with rare growths of protuberances on the lateral parts, amyloid, 22.5–34.4 × 5.4–10.6 µm. ***Cystidia*** and ***basidia*** not seen. ***Basidiospores*** ovoid with indistinct truncate apex, 10.9–12.3 × 7.3–8.5 µm (11.6 ± 0.7 × 7.9 ± 0.6 µm), IKI-, double-walled, exosporium hyaline with inter-wall pillars, endosporium yellowish brown with coarse echinulae.

Additional specimen South Africa, Western Cape Province, George, Heroldsbaai (S34° 03.249′ E22° 22.720′), at the base of dying *A. cyclops*. 13 April 2014, J.M. Tchotet Tchoumi and J. Roux, JMT124 (paratype-PREM 61937, culture ex-type CMW42149 = CBS142945). GenBank accession number: ITS = MG020248, β-tubulin = MG020153, EF1-α = MG020226.

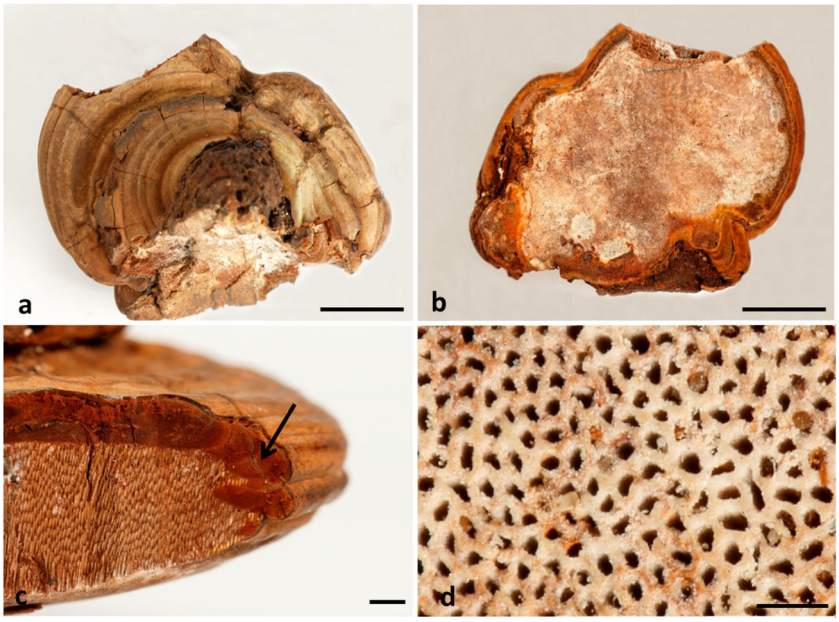

Fig. 7 *Ganoderma* sp. **a**–**b** pilear and hymenial surfaces of an immature basidiome; **c** homogenous chocolate brown context with discrete resin-like incrustations/deposits (arrowed); **d** pore surface. Bars: a-b = 2 cm; c = 2 mm; d = 1 mm

Remarks *Ganoderma dunense* and *G. destructans* cannot be distinguished from each other based on ITS phylogeny (Fig. 3). They segregate only in phylogenies for the β-tubulin and TEF1-α gene regions as well as in the combined genes (Figs. 4, 5, and 6). This phylogenetic divergence based on these three analyses is also reflected in some morphological characters. Morphologically, *G. destructans* differs from *G. dunense* in having a stipitate basidiome, a laccate shiny reddish brown pilear surface with well-developed protuberances, a not completely homogenous context, slightly smaller pores (3–5 per mm) and larger basidiospores (11–14 × 7–9 μm, Coetzee et al. 2015; Table 2).

Ganoderma dunense is macroscopically similar to *G. enigmaticum* M.P.A. Coetzee, Marinc. & M.J. Wingf., *G. aridicola* J.H. Xing & B.K. Cui and *G. austroafricanum* M.P.A. Coetzee, M.J. Wingf., Marinc. & Blanchette that also occur in South Africa and to which it is genetically related in the combined phylogeny but without statistical support (Fig. 6). They share a white poroid hymenophore surface when fresh, irregular pores and absence of black melanoid bands in the context (Crous et al. 2014; Coetzee et al. 2015; Xing et al. 2016; Table 2). However, *G. enigmaticum* and *G. aridicola* differ from *G. dunense* in their ecology. *Ganoderma enigmaticum* occurred as a parasite at the base of the trunk of *Ceratonia siliqua* L. in Pretoria, Gauteng Province (Coetzee et al. 2015), while *G. aridicola* was recovered on charred wood of *Ficus* in Durban, KwaZulu-Natal Province (Xing et al. 2016). In addition, *G. enigmaticum* differs morphologically from *G. dunense* by having a stipitate basidiome, homogenous context and narrower ellipsoid basidiospores (8–11 × 3.5–6 μm, Coetzee et al. 2015; Table 2). Similarly, *G. aridicola* differs from *G. dunense* by having a sessile basidiome, a fuscous homogenous context, distinctly stratified tube layers, smaller pores (6–8 per mm) and broadly ellipsoid basidiospores (9.7–11.2 × 7–7.8 μm, Xing et al. 2016; Table 2). *G. austroafricanum* has an annual sessile basidiome, a dimitic hyphal system and smaller (8–11 × 5.5–7 μm) subglobose basidiospores (Crous et al. 2014; Table 2).

When compared morphologically with other laccate *Ganoderma* species from South Africa and tropical Africa based on published descriptions (Steyaert 1961, 1962, 1967, 1972, 1980; Table 2), *G. dunense* shares few characteristics with most of these species. Exceptions are *G. namutambalaense* Steyaert (1962), collected in Uganda and *G. megalosporum* Steyaert (1962) collected in Kenya, which share minor similarities with *G. dunense*. They can, however, easily be distinguished from *G. dunense* in that *G. namutambalaense* has a substipitate basidiome, smaller pores and larger basidiospores, while *G. megalosporum* has larger basidiospores and much smaller sub-cylindric cuticular cells (Table 2).

Discussion

Three distinct *Ganoderma* species were found associated with dying *Acacia cyclops* trees in the Eastern and Western Cape Provinces of South Africa. Two of these species represent novel taxa but a name was provided for only one due to absence of mature basidiomes needed to describe the second species. The description of the new species brings to 11 the *Ganoderma* spp. recorded from South Africa (Van der Bijl 1921; Reid 1973, 1974, 1975; Moncalvo and Ryvarden 1997; Crous et al. 2014; Coetzee et al. 2015 and Xing et al. 2016). Of these, only five have been described with the support of DNA sequence data.

Fig. 8 *Ganoderma dunense* sp. nov. (Type, PREM 61936). **a**–**b** mature reniform-like basidiome showing a pileus surface partially covered with a dull brown deposit of basidiospores and a poroid dark brown hymenial surface; **c** pores; **d** duplex context with a light brown upper layer and a chocolate brown lower layer towards the tubes; **e** basidiospores; **f** palisade of clavi-form cutis cells; **g** skeletal hyphae; **h** skeletal hypha showing a distinct lumen (arrowed). Bars: a-b = 5 cm; c = 1 mm; d = 1 cm; e-h = 10 μm

The majority of *Ganoderma* isolates obtained in this study (33 = ~ 87%) represented *G. destructans*. This fungus was recently described as the causal agent of a serious root disease of non-native Jacaranda (*Jacaranda mimosifolia* D. Don) trees in the city of Pretoria (Tshwane Metropolitan area, Gauteng Province) in South Africa (Coetzee et al. 2015). The common occurrence of *G. destructans* on *A. cyclops* in the Western Cape, together with its occurrence on *J. mimosifolia* more than 1000 km further north in the country suggests that it has a wide host range, but also a wide geographical distribution. Coetzee et al. (2015) suggested that this fungus might be a native species and *A. cyclops* thus represents the second non-native host that it has successfully colonized. Its wide geographic distribution also supports the contention that it is a native South African fungus.

The two novel species of *Ganoderma* obtained from *A. cyclops* in this study were represented by only five isolates. Two were of the *Ganoderma* sp. that was not described and three were of the newly described *G. dunense*. Based on the appearance of the pilear surface, *G. dunense* could be linked to the *G. lucidum* complex, while the undescribed *Ganoderma* sp. was related to species in the *G. applanatum* complex (Imazeki 1952; Richter et al. 2015).

As has been found in many other studies (i.e. Gottlieb et al. 2000 and Zhou et al. 2015) sequence data for the ITS gene regions were not sufficient to delineate between *G. dunense* and *G. destructans*. Based on the ITS phylogeny, *G. dunense* would be treated as the same as *G. destructans*. But phylogenies inferred from the β-tubulin and TEF1-α data sets, as well as that of the combined genes, showed that this taxon represented a novel species. Morphological characterization also

Table 2 Morphological comparison of *G. dunense* sp. nov. with other laccate *Ganoderma* taxa found in South Africa and tropical Africa

Taxon	Shape	Pores/mm	Spores (µm)	Cutis	Other	Reference
Ganoderma africanum	NI	NI	NI	NI	type not found	Moncalvo and Ryvarden 1997
G. aridicola	sessile dimidiate, pilear surface fuscous black when fresh, reddish brown to black upon drying	6–8	9.7–11.2 × 7–7.8, broadly ellipsoid	amyloid elements 30–55 × 5–8 µm	skeletal hyphae up to 2.5–5 µm wide	Xing et al. 2016
G. austroafricanum	sessile, dimidiate	3–4	8–11 × 5.5–7 broadly ellipsoid	NI	NI	Crous et al. 2014
G. capensis	sessile	5–6	9.75–10.5 × 5.75–6.2	elements 50 × 5–10 µm up to 9–12 µm when capitate	dimitic hyphal system	Reid 1975
	–	6	10–12 × 6–7 ovoid to ellipsoid	amyloid elements 35–45(−55) × 7–9 µm	trimitic with skeleteo-binding hyphae, skeletal hyphae 5.5–10 µm diam.	This publication
G. destructans	stipitate globular pileus	3–5	11–14 × 7–9	amyloid elements 13–35 × 4.5–7.5	homogeneous context	Coetzee et al. 2015
	laccate shiny reddish brown, stipe lateral to eccentric and circular to ellipsoid, pileus dimidiate to circular, with small to wide protuberances		–	–	not completely homogeneous context	This publication
G. dunense sp. nov.	sessile but with a lateral mucro, pileus dimidiate or reniform	3–4	10.9–12.3 × 7.3–8.5	amyloid elements clavate, 22.5–34.4 × 5.4–10.6 µm	duplex context present	This publication
G. enigmaticum	stipitate globular pileus	3–5	8–11 × 3.5–6	amyloid elements 20–46 × 5.5–9 µm	–	Coetzee et al. 2015
G. hildebrandii	small basidiome centrally stipitate	7–8	7–8(8.5) × 4.5–5.5(−6)	IKI–elements similar but wider up to 15 µm	dextrinoid skeletal hyphae	Moncalvo and Ryvarden 1995, 1997
G. reticulatosporum	centrally stipitate pileus, umbrella shaped	3–4	25–26 × 15.5–16	NI	perhaps *Humphreya* sp.	Reid 1973 Moncalvo and Ryvarden 1997
G. namutambalaense	substipitate flabellate	5–6	11.5–14 × 8–9.5	elements sphaeropedunculate, 50 × 4–7(−10) µm, sustaining hyphae 2–3 µm	from Uganda	Steyaert 1962
G. megalosporum	sessile dimidiate	3–4	11.5–13 × 8–9	elements subcylindric 30 × 4–6 µm	from Kenya	Steyaert 1962

NI refers to no information in the literature

revealed very distinct macro- and microscopic characters that could further distinguish between these two taxa.

In the global multi-locus phylogeny, *G. dunense* formed a well-resolved and isolated monophyletic clade. However, it was linked to species belonging to the *G. lucidum* complex (Li et al. 2015; Zhou et al. 2015; Richter et al. 2015) but without these relationships being statistically supported. These species included *G. enigmaticum*, *G. aridicola*, *G. carnosum*, *G. lucidum* (*s. lat.*), *G. leucocontextum*, *G. tsugae*, *G. oregonense*, *G. austroafricanum*, *G. resinaceum* and *G. sessile*. Although the placement of *G. dunense* among these species lacked statistical support, it indicates a relatedness to species in the complex, which was also supported by its morphology.

The extent of infection by *Ganoderma* species in this study raises an intriguing question about the role of *P. acaciicola* in the death of *A. cyclops*. More specifically, whether it is the only causal agent of the deaths of these trees as reported by Wood and Ginns (2006). This question is worth considering because most of the isolates recovered from recently infected trees in the current study were of *G. dunense* and only a single isolate was identified as *P. acaciicola*. Moreover, although *Ganoderma* was included in the pathogenicity trials conducted by Wood and Ginns (2006), results of the present study show that at least three species of *Ganoderma* are associated with the dying *A. cyclops* in these areas. It is not known which of the three *Ganoderma* species was used in the aforementioned trials. Additionally, most of the sampled trees exhibited symptoms typical of Ganoderma root rot similar to those observed in previous studies (Glen et al. 2009; Coetzee et al. 2011). It is, therefore, clear that further investigations should be undertaken to determine the role of *P. acaciicola* and *Ganoderma* species in the death of *A. cyclops* trees in the coastal areas of South Africa.

Acknowledgements We thank the Department of Science and Technology (DST), the National Research Foundation (NRF) and the International Cooperation Program (MINCYT-Argentina – DST-South Africa, SA/10/02) for funding.

References

Avis AM (1989) A review of coastal dune stabilization in the Cape Province of South Africa. Landsc Urban Plan 18:55–68

Bishop KS, Kao CHJ, Xu Y, Glucina MP, Paterson RRM, Ferguson LR (2015) From 2000 years of *Ganoderma lucidum* to recent developments in nutraceuticals. Phytochemistry 114:56–65

Coetzee MPA, Wingfield BD, Golani GD, Tjahjono B, Gafur A, Wingfield MJ (2011) A single dominant *Ganoderma* species is responsible for root rot of *Acacia mangium* and *Eucalyptus* in Sumatra. South For 73:175–180

Coetzee MPA, Marincowitz S, Muthelo VG, Wingfield MJ (2015) *Ganoderma* species, including new taxa associated with root rot of the iconic *Jacaranda mimosifolia* in Pretoria, South Africa. IMA Fungus 6:249–256

Crous PW, Wingfield MJ, Schumacher RK, Summerell BA, Giraldo A, Gené J, Guarro J, Wanasinghe DN, Hyde KD, Camporesi E, Garethjones EB, Thambugala KM, Malysheva EF, Malysheva VF, Acharya K, Álvarez J, Alvarado P, Assefa A, Barnes CW, Bartlett JS, Blanchette RA, Burgess TI, Carlavilla JR, Coetzee MPA, Damm U, Decock CA, Denbreeÿen A, Devries B, Dutta AK, Holdom DG, Rooney-Latham S, Manjón JL, Marincowitz S, Mirabolfathy M, Moreno G, Nakashima C, Papizadeh M, Shahzadehfazeli SA, Amoozegar MA, Romberg MK, Shivas RG, Stalpers JA, Stielow B, Stukely MJC, Swart WJ, Tan YP, Vanderbank M, Wood AR, Zhang Y, Groenewald JZ (2014) Fungal planet description sheets: 281–319. Persoonia 33:212–289

Darriba D, Taboada GL, Doallo R, Posada D (2012) jModelTest 2: more models, new heuristics and parallel computing. Nat Methods 9:772

Douanla-Meli C, Langer E (2009) *Ganoderma carocalcareus* sp. nov., with crumbly-friable context parasite to saprobe on *Anthocleista nobilis* and its phylogenetic relationship in *G. resinaceum* group. Mycol Prog 8:145–155

Flood J, Bridge PD, Holderness M (eds) (2000) Ganoderma diseases of perennial crops. CABI Publishing, Wallingford, p 275

Gill AM (1985) *Acacia cyclops* G. Don (Leguminosae: Mimosaceae) in Australia: distribution and dispersal. J R Soc West Aust 67:59–65

Gill W, Eyles A, Glen M, Mohammed C (2016) Structural host responses of *Acacia mangium* and *Eucalyptus pellita* to artificial infection with the root rot pathogen, *Ganoderma philippii*. Forest Pathol 46:369–375

Glen M, Bougher NL, Francis AA, Nigg SQ, Lee SS, Irianto R, Barry KM, Beadle CL, Mohammed CL (2009) *Ganoderma* and *Amauroderma* species associated with root-rot disease of *Acacia mangium* plantation trees in Indonesia and Malaysia. Australas Plant Pathol 38:345–356

Gottlieb AM, Ferrer E, Wright JE (2000) rDNA analyses as an aid to the taxonomy of species of *Ganoderma*. Mycol Res 104:1033–1045

Henderson L (1998) Invasive alien woody plants of the southern and southwestern cape region, South Africa. Bothalia 28:91–112

Henderson L (2007) Invasive, naturalized and casual alien plants in southern Africa: a summary based on the Southern African plant invaders atlas (SAPIA). Bothalia 37:215–248

Hong SG, Jung HS (2004) Phylogenetic analysis of *Ganoderma* based on nearly complete mitochondrial small-subunit ribosomal DNA sequences. Mycologia 96:742–755

Imazeki R (1952) A contribution to the fungus flora of Dutch New Guinea. Bull Gov Forest Exp Sta, Meguro. Tokyo 57:87–128

Katoh K, Standley DM (2013) MAFFT multiple sequence alignment software version 7: improvements in performance and usability. Mol Biol Evol 30:772–780

Kauserud H, Schumacher T (2001) Outcrossing or inbreeding: DNA markers provide evidence for type of reproductive mode in *Phellinus nigrolimitatus* (Basidiomycota). Mycol Res 53:220–230

Kinge TR, Mih AM (2011) *Ganoderma ryvardense* sp. nov. associated with basal stem rot (BSR) disease of oil palm in Cameroon. Mycosphere 2:179–188

Kinge TR, Mih AM, Coetzee MPA (2012) Phylogenetic relationships among species of *Ganoderma* (Ganodermataceae, Basidiomycota) from Cameroon. Aust J Bot 60:526–538

Kirk PM, Cannon PF, Minter DW, Stalpers JA (2008) Dictionary of the fungi, 10th edn. CAB International, Wallingford

Kotzé LJD, Wood AR, Lennox CL (2015) Risk assessment of the *Acacia cyclops* dieback pathogen, *Pseudolagarobasidium acaciicola*, as a mycoherbicide in south African strandveld and limestone fynbos. Biol Control 82:52–60

Li TH, Hu HP, Deng WQ, Wu SH, Wang DM, Tsering T (2015) *Ganoderma leucocontextum*, a new member of the *G. lucidum* complex from Southwestern China. Mycoscience 56:81–85

Miller MA, Pfeiffer W, Schwartz T (2010) Creating the CIPRES Science Gateway for inference of large phylogenetic trees in Proceedings of

the Gateway Computing Environments Workshop (GCE), 14 Nov. 2010, New Orleans, LA pp 1–8

Möller EM, Bahnweg G, Sandermann H, Geiger HH (1992) A simple and efficient protocol for isolation of high molecular weight DNA from filamentous fungi, fruit bodies, and infected plant tissues. Nucleic Acids Res 20:6115–6116

Moncalvo JM, Ryvarden L (1995) Ganoderma hildebrandii, a forgotten species. Mycotaxon 56:175–180

Moncalvo JM, Ryvarden L (1997) A nomenclatural study of the Ganodermataceae Donk. Synopsis Fungorum 11. Fungiflora, Oslo

Park Y, Kwon O, Son E, Yoon D, Han W, Yoo Y, Lee C (2012) Taxonomy of *Ganoderma lucidum* from Korea based on rDNA and partial β-tubulin gene sequence analysis. Mycobiology 40:71–75

Paterson RRM (2007) Ganoderma disease of oil palm-a white rot perspective necessary for integrated control. Crop Prot 26:1369–1376

Ramasamy S (1972) Cross-infectivity and decay ability of *Ganoderma* species parasitic to rubber, oil palm and tea. In: Ganoderma diseases of perennial crops. Flood J, Bridge PD and Holderness M, 2000. CABI, Wallingford, UK

Reid DA (1973) A reappraisal of type and authentic specimens of Basidiomycetes in the van der Byl herbarium, Stellenbosch. S Afr J Bot 39:141–178

Reid DA (1974) A reappraisal of type and authentic material of the larger Basidiomycetes in the Pretoria Herbarium. Bothalia 11:221–230

Reid DA (1975) Type studies of the larger Basidiomycetes described from southern Africa. Contributions from the Bolus Herbarium 7: 1–255

Richter C, Wittstein K, Kirk P, Stadler M (2015) An assessment of the taxonomy and chemotaxonomy of *Ganoderma*. Fungal Divers 71: 1–15

Ronquist F, Teslenko M, van der Mark P, Ayres DL, Darling A, Höhna S, Larget B, Liu L, Suchard MA, Huelsenbeck JP (2012) MrBayes 3.2: efficient Bayesian phylogenetic inference and model choice across a large model space. Syst Biol 61:539–542

Ryvarden L, Melo I (2014) Poroid fungi of Europe. Synopsis Fungorum 31:1–455

Shackleton CM, McConnachie M, Chauke MI, Mentz J, Sutherland F, Gambiza J, Jones R (2006) Urban fuelwood demand and markets in a small town in South Africa: livelihood vulnerability and alien plant control. Int J Sustain Dev World Ecol 13:481–491

Silvestro D, Michalak I (2012) raxmlGUI: a graphical front-end for RAxML. Org Divers Evol 12:335–337

Stamatakis A (2006) RAxML-VI-HPC: maximum likelihood-based phylogenetic analyses with thousands of taxa and mixed models. Bioinformatics 22:2688–2690

Steyaert RL (1961) Genus *Ganoderma* (Polyporaceae) taxa nova — I. In Bulletin du Jardin Botanique de l'État à Bruxelles 31:69–83

Steyaert RL (1962) Genus *Ganoderma* (Polyporaceae) taxa nova—2. In Bull du Jard Bot Natl Belgique 32:89–104

Steyaert RL (1967) Les *Ganoderma palmicoles*. Bull du Jard Bot Natl Belgique 37:465–492

Steyaert RL (1972) Species of *Ganoderma* and related genera mainly of the Bogor and Leiden Herbaria. Persoonia 7:55–118

Steyaert RL (1980) Study of some *Ganoderma* species. Bull du Jard Bot Natl Belgique 50:135–186

Swofford DL (2002) PAUP*: phylogenetic analysis using parsimony (*and other methods). Version 4. Sinauer Associates, Sunderland

Tamura K, Peterson D, Peterson N, Stecher G, Nei M, Kumar S (2011) MEGA 5: molecular evolutionary genetics analysis using maximum likelihood, evolutionary distance, and maximum parsimony methods. Mol Biol Evol 28:2731–2739

Taylor H (1969) Pest plants and nature conservation in the winter rainfall region. J Bot Soc South Africa 55:32–35

Van der Bijl PA (1921) A contribution to our knowledge of the Polyporeae of South Africa. S Afr J Sci 18:246–293

White TJ, Bruns T, Lee S, Taylor J (1990) Amplification and direct sequencing of fungal ribosomal RNA genes for phylogenetics. In: Innis MA, Gelfand DH, Sninsky JJ, White TJ (eds) PCR protocols: a guide to methods and applications. Academic Press, New York, pp 315–322

Wood AR, Ginns J (2006) A new dieback disease of *Acacia cyclops* in South Africa caused by *Pseudolagarobasidium acaciicola* sp. nov. Can J Bot 84:750–758

Worrall JJ (1991) Media for selective isolation of hymenomycetes. Mycologia 83:296–202

Xing JH, Song J, Decock C, Cui BK (2016) Morphological characters and phylogenetic analysis reveal a new species within the *Ganoderma lucidum* complex from South Africa. Phytotaxa 266: 115–124

Zhou LW, Cao Y, Wu SH, Vlasák J, Li DW, Li MJ, Dai YC (2015) Global diversity of the *Ganoderma lucidum* complex (Ganodermataceae, Polyporales) inferred from morphology and multilocus phylogeny. Phytochemistry 114:7–15